



21st IAEA Fusion Energy Conference
Chengdu, China, 16 - 21 October, 2006

IAEA-CN-149/ TH/P6-17

Two-dimensionally Steep Structure of the Electric Field in Tokamak H-mode

N. Kasuya and K. Itoh

NIFS-861

Oct. 2006

Two-dimensionally Steep Structure of the Electric Field in Tokamak H-mode

N. Kasuya 1), K. Itoh 1)

1) National Institute for Fusion Science, Toki, Gifu 509-5292, Japan

e-mail contact of main author: kasuya@nifs.ac.jp

Abstract. The rapid formation of a density pedestal on an L/H transition has been raising a question why the rapid density evolution is induced. Formation of a poloidal shock structure is predicted in H-mode transport barriers, and consideration of the two-dimensional structure both in the radial and poloidal directions is inevitable to clarify the formation mechanism of the H-mode pedestal. The analyses are carried out with edge plasmas in tokamak H modes, which are induced either spontaneously or by electrode biasing. Two-dimensional structures of the potential, density and flow velocity are calculated with the momentum conservation equation. The validity of the one-dimensional L/H transition theory and the iterative process to obtain the two-dimensional structure are confirmed by our analysis. A steep electric field structure both in the radial and poloidal directions is obtained. The two-dimensional electric field induces radial ion fluxes, which increase in the H-mode transport barrier and affect the electric field. If the Boltzmann relation is violated, radial electron fluxes are induced, and affect the density evolution. Reduction of anomalous transport by the steep gradient of the radial electric field, and generation of the particle fluxes associated with the two-dimensional structure influence the rapid formation of the steep gradients in H-mode plasmas. A transport model including both effects is constructed to reveal the self-consistent mechanism of the density pedestal formation in the L/H transition.

1. Introduction

Researches on tokamak high-confinement-mode (H-mode) [1] physics have been greatly developed [2], but there remain unresolved problems. One of the problems is the rapid formation mechanism of a density pedestal on a low to high confinement mode (L/H) transition [3]. Formation of a poloidal shock structure is predicted in the H-mode transport barrier [4,5], and existence of the poloidal electric field induces an $E \times B$ convective particle flux in the radial direction [2]. Therefore, consideration of the two-dimensional (2-D) structure both in the radial and poloidal directions is inevitable to clarify the formation mechanism of the H-mode pedestal. In this paper, 2-D electric field structures are studied by extending the one-dimensional (1-D) model in tokamak H modes. The analyses show that the poloidal electric field, formed in the H-mode transport barrier, generates convective particle fluxes, which is firstly calculated with consideration of the 2-D structural formation. A transport model including the 2-D effect is constructed to reveal the self-consistent mechanism of the density pedestal formation on the L/H transition.

2. Model Equation

The theoretical framework for describing bifurcation of the radial structure as well as poloidal inhomogeneity in tokamak edge plasmas is based on the momentum balance equation [6]. The flux-surface-averaged poloidal component of the momentum balance can be simplified to be

$$J = \Gamma_{\text{bulk}} + \Gamma_{\text{shear}}, \quad (1)$$

where J is the radial current, Γ_{bulk} and Γ_{shear} are ion fluxes driven by neoclassical [7] and anomalous processes [2], respectively. Equation (1) can be written to be

$$\frac{\partial}{\partial t} E_r = -\frac{1}{\epsilon_0 \epsilon_{\perp}} (J_{\text{visc}} + J_r - J_{\text{ext}}), \quad (2)$$

where ε_0 is the vacuum susceptibility, ε_{\perp} is the dielectric constant of a magnetized plasma, J_{visc} , J_r and J_{ext} are the current driven by anomalous shear viscosity of ions, neoclassical bulk viscosity, and external component as an electrode, orbit loss, etc., respectively [8]. Term J_{visc} , J_r and the other terms come from Γ_{shear} , Γ_{bulk} and J in Eq. (1), respectively. The time evolution of the poloidal Mach number M_p , which is related to the radial electric field, is obtained from Eq. (2).

The shock ordering $\chi = \ln(n/n_0) = O(\varepsilon^{1/2})$ [5] can be used where ε is the inverse aspect ratio, because the large M_p case is considered as in H modes. The inverse aspect ratio ε is considered to be small. We assume that the radial flow velocity V_r is much smaller than the poloidal flow velocity V_p . By these ordering and assumption, the equation that determines the poloidally-symmetric part of the electric field, Eq. (2), is decoupled with that governs the poloidally-asymmetric part $\chi(r, \theta)$. The parallel component of the momentum balance gives the equation for χ with given M_p to be

$$\begin{aligned} M_p \exp(-\chi) \frac{\partial \chi}{\partial \tau_p} = & -\hat{\mu} r^2 \frac{B_0}{B_p} \frac{\partial^2}{\partial r^2} \{M_p [\exp(-\chi) - 1]\} \\ & + \frac{2}{3} D \exp(-\chi) \frac{\partial^2 \chi}{\partial \theta^2} + (1 - M_p^2) \frac{\partial \chi}{\partial \theta} + 2A \frac{\partial \chi^2}{\partial \theta} - \left(\chi - \frac{\chi^2}{2} + 2\varepsilon \cos \theta \right) \frac{\partial M_p}{\partial \tau_p}, \quad (3) \\ & - \varepsilon \left\{ \left[D - \hat{\mu} \frac{B_0}{B_p} \left[2r^2 \frac{\partial^2 M_p}{\partial r^2} + 4r \frac{\partial M_p}{\partial r} - 2M_p \right] \right] \cos \theta - 2M_p^2 \sin \theta \right\} \end{aligned}$$

where $M_p = KB_0 / (\bar{n} v_{ti} C_r)$, $K = nV_p / B_p$, $\tau_p = t/t_p$, $t_p = B_0 r / (B_p v_{ti} C_r)$, $v_{ti} = \sqrt{2T_i/m_i}$, $\hat{\mu} = \mu / (r v_{ti} C_r)$, $A = M_p^2 / 2 + 5 / (36 C_r^2)$, $C_r^2 = 5/6 + T_e / (2T_i)$, $D = 4\sqrt{\pi} I_{ps} KB_0 / (3\bar{n} v_{ti} C_r^2)$, B_0 is the toroidal magnetic field at the magnetic axis, B_p is the poloidal magnetic field, $n = n_i = n_e$ is the density, m_i is the ion mass, μ is the shear viscosity coefficient, and T_i and T_e is the temperature of ion and electron, respectively. τ_p is the time normalized by t_p , which is of the order of the duration for which the particle with the thermal velocity completes one poloidal rotation, so the time scale of 2-D structural formation is given by this poloidal transit time t_p . The form of I_{ps} is represented in Eq. (10) of Ref. [5], and depends on M_p and the collision frequency [9].

Time evolution of the 2-D structure is calculated from Eq. (3) by substituting M_p obtained by Eq. (2). Then, using Boltzmann relation

$$n = \bar{n} \exp \frac{e\Delta\Phi}{T_i}, \quad (4)$$

χ is directly related to the potential perturbation, and the potential profile is obtained, where \bar{f} and Δf represent the spatial average and perturbed parts of quantity f , respectively. This iterative process is appropriate, because a condition $V_r / V_p \ll 1$ is satisfied, even if a strong poloidal shock exists [6].

3. Two-dimensional Electric Field Structure

This section provides the electric field structures obtained from the 2-D model in Sec. 2. The analyses are carried out with edge plasmas in tokamak H modes, which are induced either spontaneously or by electrode biasing, to show the 2-D steep structural formation.

3.1. Geometry

Analyses are carried out in the region near the plasma edge, $r = (a - d) \sim a$, where $r = a$ is

the position of the last closed flux surface, and d is the width of the region (between the surfaces S1 and S2 in Fig. 1). For studying the impact of a biasing-limiter, the externally applied voltage V_{ext} is imposed between the surfaces S1 and S2 connected by an external circuit with resistance \hat{r} . On the other hand, there is no external circuit for spontaneously obtained H modes, which is induced by large gradients of the density and temperature. We choose the boundary condition to be $\chi = 0$ at $r = (a - d)$ and a . This is an idealization, considering that no perturbation exists outside of this region (such as in the edge barrier or biased region). The boundary condition for M_p is set to be $\partial M_p / \partial r = 0$ at $r = (a - d)$ and a . The following parameter set is used for the calculation in this paper: $R = 1.75$ [m], $a = 0.46$ [m], $B_0 = 2.35$ [T], $T_i = 40$ [eV], $I_p = 200$ [kA] and $d = 5$ [cm].

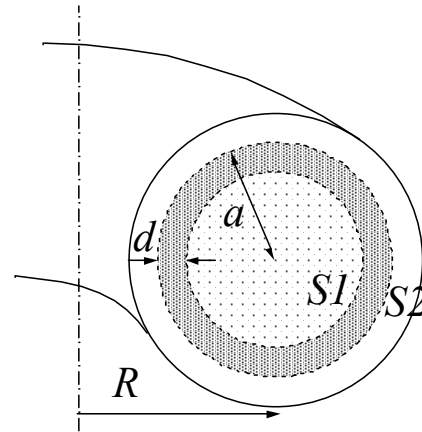


FIG. 1. Schematic of the edge plasma (poloidal cross section). The analyses are carried out in the region between the surface S1 and S2.

3.2. H mode Induced by Externally Applied Voltage

The first example of the calculation is given for the electrode-biasing H mode. Nonlinear formation mechanisms of the steep radial electric field structure have been studied by biased limiter experiments in which an externally driven H-mode transition was induced [10,11]. Imposing a radial electric field by an electrode inserted into a plasma gives a transition to an improved confinement state when the applied voltage between the electrode and the limiter is larger than a threshold value. This transition is characterized by a sudden change of the radial electric field structure from a flat one to a peaked one (solitary structure) [8,12]. A steep electric field structure both in the radial and poloidal directions is obtained by using a plasma parameter set in the electrode-biasing H mode. Potential profiles in the radial direction are represented in Fig. 2, where the solutions of the 1-D (flux-surface averaged) [8] and 2-D model are shown. The steep radial gradients show almost the same feature, so the 1-D model can represent the characteristic radial structure in the H mode. In

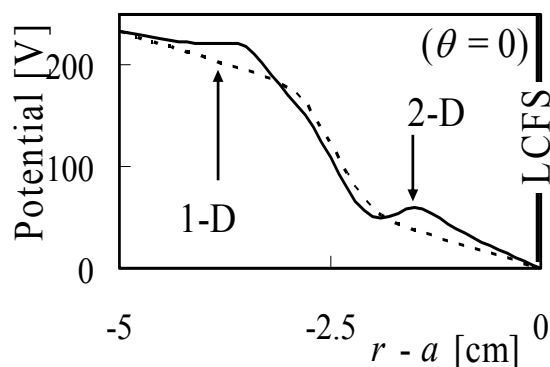


FIG. 2. Radial profiles of the potential at $\theta = 0$ in the electrode-biasing H mode (Solutions of the 1-D and 2-D model).

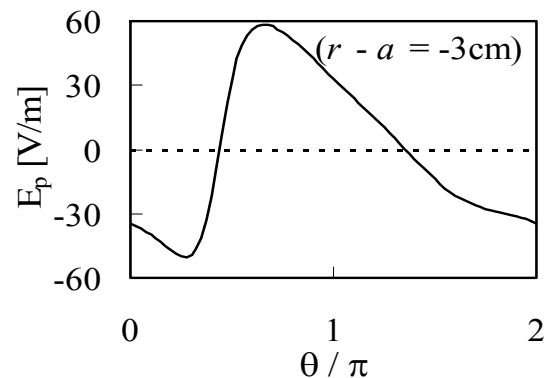


FIG. 3. Poloidal profile of the poloidal electric field at $r - a = -3$ [cm] in electrode-biasing H mode. The poloidal shock structure is formed at $\theta \sim 0.5\pi$.

addition, there exists a poloidal structure. Figure 3 shows a poloidal electric field profile. A steep gradient in the poloidal direction (poloidal shock) exists at $\theta \sim 0.5\pi$. The position of the shock structure depends on the magnitude of the poloidal Mach number, and appears at $\theta = 0$ when $M_p = 1$ [5]. This poloidal inhomogeneity induces an $E \times B$ convective particle flux in the radial direction as will be discussed in Sec. 5.

3.3. Spontaneous H Mode

The analysis is also performed for the case of the spontaneous H mode driven by ion-orbit losses [13,14]. The radial electric field often has the negative sign in the spontaneous H modes, and the solitary structure is not accessible [8]. The origin of the bifurcation in our model is nonlinearity of the bulk-ion-viscosity term and the ion-orbit-loss term. These terms have nonlinear responses to the radial electric field, and a large density gradient, which induces a large ambipolar electric field, can give a large radial electric field. With a prescribed inhomogeneous density profile as shown in Fig. 4 (a), normal and enhanced radial electric field branches are taken in the small and large gradient regions (near the

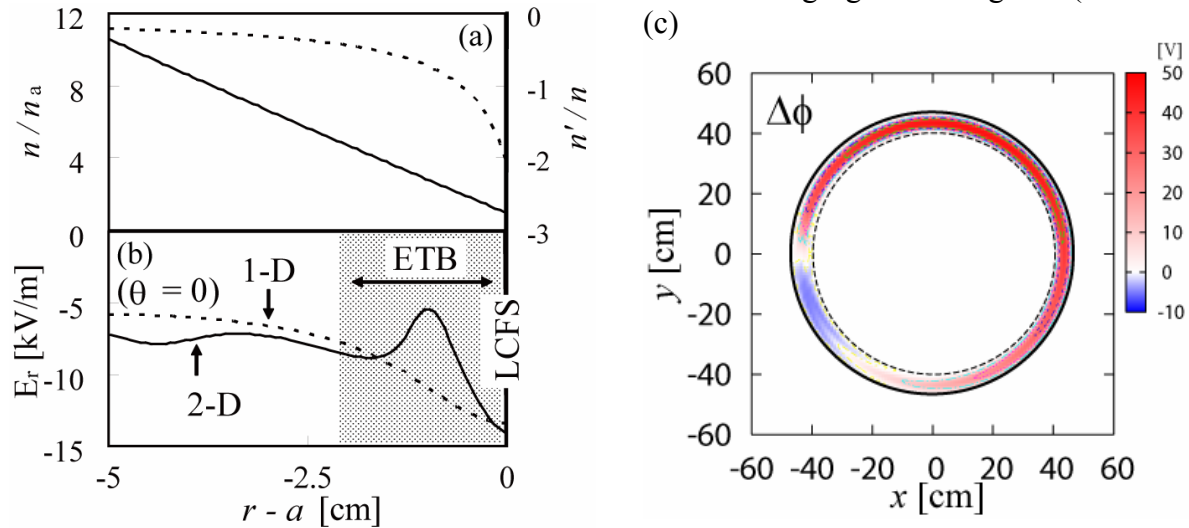


FIG. 4. (a) Radial profiles of the density (n) normalized by the density at $r = a$ (n_a), and the reciprocal of the density scale length. (b) Radial profiles of the radial electric field at $\theta = 0$ (Solutions of the 1-D and 2-D model), and (c) 2-D structure of the potential perturbation in the spontaneous H mode.

boundary $r - a = -5, 0$ [cm]), respectively, and a critical layer is formed between these regions (at $r - a \sim -1$ [cm]). The steep gradient of the radial electric field is formed in this layer. The width of the layer depends on the shear viscosity coefficient [2]. The radial electric field profiles in the radial direction are shown in Fig. 4 (b) by solving the 1-D and 2-D model. The 2-D structure of the potential perturbation is shown in Fig. 4 (c). There exists a poloidal structure in the same way with the electrode biasing case. Figure 5 shows the poloidal electric field profile. The poloidal shock structure exists at $\theta \sim 0.2\pi - 0.5\pi$ in this case.

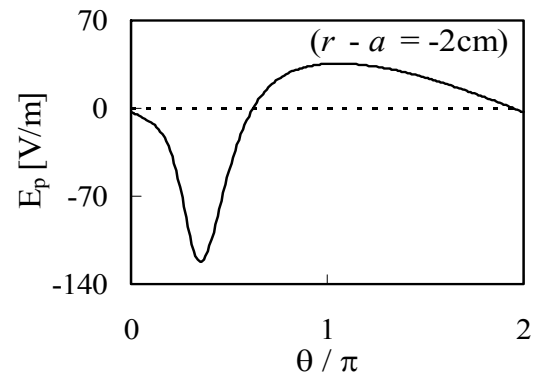


FIG. 5. Poloidal profile of the poloidal electric field at $r - a = -2$ [cm] in spontaneous H mode. The poloidal shock structure is formed at $\theta \sim 0.2\pi - 0.5\pi$.

4. Self-consistent Transport Model Including the Two-dimensional Effect

As shown in the previous section, a 2-D electric field is formed in the H-mode transport barriers induced both spontaneously and by electrode biasing in the plasma edge region. The poloidal electric field generates an $E \times B$ convective flow in the radial direction, so the flux-surface-averaged radial flux is calculated to estimate its effect on particle transport.

The $E \times B$ drifts of ions and electrons direct to the same direction, depending on the sign of the radial electric field, the toroidal magnetic field and the plasma current [9]. Adding the diamagnetic flow with electrons which satisfied the Boltzmann relation on the same flux surface, the electron radial flux is canceled to be zero. On the other hand, the ion radial flux is generated, and its particle velocity is more than 1 [m/s] in the transport barrier region. This radial ion flux affects the radial electric field by contributing to the radial current in Eq. (1) to be

$$\frac{\partial}{\partial t} E_r = -\frac{1}{\varepsilon_0 \varepsilon_{\perp}} (J_{\text{visc}} + J_r + J_p - J_{\text{ext}}), \quad (5)$$

$$J_p = e \left(1 + \frac{T_i}{T_e} \right) \left\langle \frac{n E_p}{B} \right\rangle, \quad (6)$$

where J_p is the additional current arising from the 2-D effect, and $\langle \rangle$ denotes the flux surface average.

The radial electron flux is zero with the Boltzmann relation, so it does not affect directly to the density pedestal formation as described in Ref. [9]. If there is a mechanism to violate the Boltzmann relation of electrons, such as electron-ion collisions, the 2-D structure contributes to the radial electron flux. Here, we introduce this 2-D effect deductively by using the phase delay δ between the potential and the density to be

$$\Gamma_e = \frac{n E_p}{B} [1 - \exp(-i\delta)]. \quad (7)$$

The phase delay δ is taken as a prescribed parameter in this paper, and the estimation of this value will be carried out in a future work.

Taking into consideration of the ion and electron radial fluxes, the transport model including the 2-D effect is explained. The structure of the transport model is described in Fig. 6. There are two kinds of driving force; one is the external drive V_{ext} , which is the imposed biasing voltage taken as a control parameter in the case of the electrode-biasing H mode, and the other is the internal drive α , which is the temperature gradient taken as a control parameter in the case of the spontaneous H mode. The internal drive is modeled in the ambipolar electric field X_a as

$$X_a = \rho_p \left(\frac{1}{n} \frac{\partial n}{\partial r} + \alpha \right), \quad (8)$$

where ρ_p is the poloidal Larmor radius. A control of these driving parameters changes the radial electric field, which is obtained by solving Eq. (5), and an L/H transition is taken place. The large radial electric field forms a 2-D electric field, which is obtained by solving Eq. (3) with the substitution of M_p . Then, particle fluxes Γ_i and Γ_e are induced. The ion flux Γ_i contributes to the radial current in Eq. (5) and the electron flux Γ_e given by Eq. (7) contributes to the convective component in the continuity equation written as

$$\frac{\partial n}{\partial t} = -\nabla(nV - D_a \nabla n) + S, \quad (9)$$

where V , D_a and S are the flow velocity, diffusion coefficient and particle source, respectively. The density profile is reflected into the ambipolar electric field X_a (Eq. (8)). In this way, a self-consistent loop is closed in our transport model.

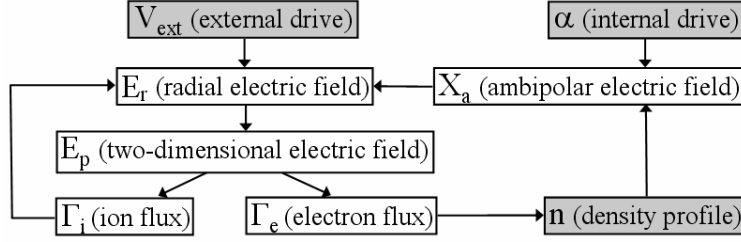


FIG. 6. Structure of the transport code including the 2-D electric field effect.

5. Time Evolution on the L/H Transition

Using the model including the 2-D effect, a self-consistent density evolution in an L/H transition is calculated. Figure 7 shows time evolutions of the poloidal Mach number, which corresponds to the radial electric field, and the density, when α is ramped up at $t = 0$ from 0.0 to -0.45 in the duration of 100 μs . This is the case with $\delta = 0$. The diffusion coefficient D_a is modeled to be reduced from 1.0 [m^2/s] to 0.2 [m^2/s] at $t = 0$ corresponding to the suppression of anomalous transport. The negative radial electric field changes its profile from a flat one (L mode) to that larger near the last closed flux surface (H mode). The radial profile of the H-mode state is similar to that shown in Fig. 4. The 2-D electric field changes in accordance with the evolution of M_p , and the large poloidal electric field generates an $E \times B$ flow pointing to the radial direction. Figure 8 shows the flux-surface-averaged convective velocity of the $E \times B$ flow. The radial profiles of the convective velocity in the steady L- and H-mode states are shown. The convective velocity is inhomogeneous in radius, and increases in accordance with the increase of M_p . The final state has the maximum value of $\langle V_{E \times B} \rangle = 7$ [m/s]. This flux affects the electric field by generating the radial current J_p . In the spontaneous L/H transition, the current J_p has the same order of magnitude of the bulk viscosity current and the orbit loss current, so it must be taken account for obtaining a threshold of the L/H transition. Note that, in the electrode biasing case, J_r is much larger than J_p , ($J_p / J_r = 0.1$ in the L mode and 0.3 in the H mode in the positive biasing case in Fig. 2), so the effect on the magnitude of the radial electric field is smaller than that in the spontaneous transition.

The electron radial flux arising from the 2-D effect is discussed next. The direction of the convection depends on the direction of the radial electric field, the toroidal magnetic field and the plasma current. In the spontaneous H mode with a negative radial electric field,

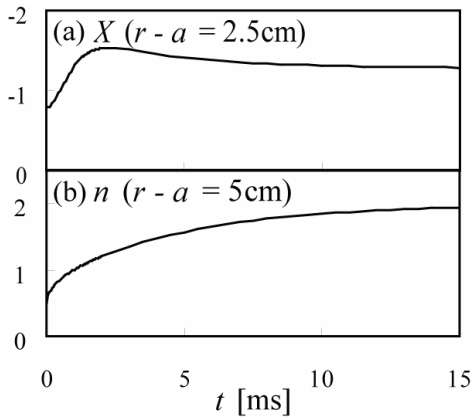


FIG. 7. Time evolution of (a) the radial electric field at $r - a = 2.5$ [cm] and (b) the density at $r - a = 5$ [cm] on the L/H transition with $\delta = 0$.

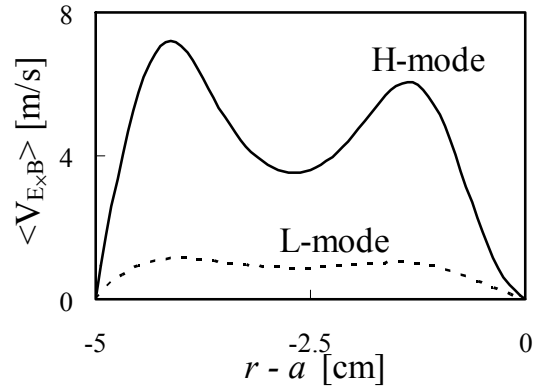


FIG. 8. Radial profiles of the flux-surface-averaged particle flux driven by the poloidal electric field in the cases of the L and H mode in Fig. 7.

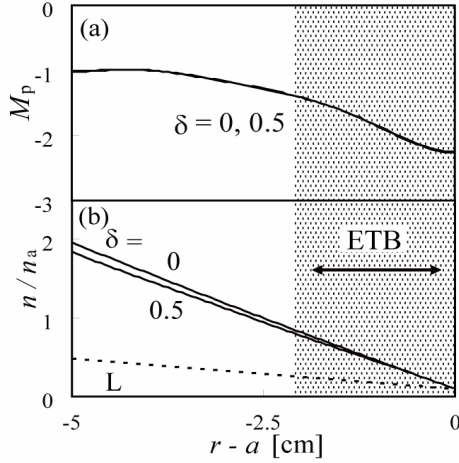


FIG. 9. (a) Radial profiles of the poloidal Mach number and (b) the density in the H mode. The cases with $\delta = 0$ and 0.5 are shown. The density profile in the L mode is also indicated by the dashed curve.

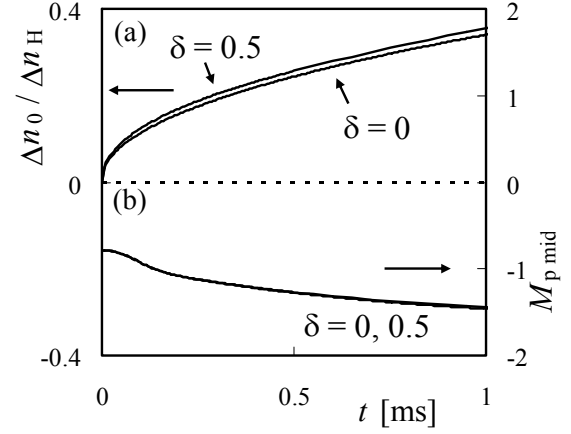


FIG. 10. Time evolution of (a) the density increase at $r - a = -5$ [cm] and (b) the poloidal Mach number at $r - a = -2.5$ [cm] after the α ramp up. The cases with $\delta = 0$ and 0.5 are shown.

when the toroidal magnetic field and the plasma current point to the same directions, the convective velocity directs outward. With the existence of the phase delay between the potential and the density, the radial electron flux is not zero and can affect the formation of the density pedestal. Figure 9 shows the profiles of the poloidal Mach number and the density with $\delta = 0$ and 0.5 . The value $\delta = 0.5$ is chosen as a representative for a small but finite value of δ . The conditions are same with the steady state in Fig. 7 except for the value of δ . There is little difference in the M_p profiles with different δ (less than few %, between the cases with $\delta = 0$ and 0.5). This is consistent with the procedure when M_p and χ are solved in the limit with $\delta = 0$. The boundary conditions of the density are set to be constant particle flux at $r - a = -5$ (inner boundary) and constant density at $r - a = 0$ (outer boundary). With these boundary conditions, the density decreases with larger δ (large convective particle flux) as shown in Fig. 9 (b). In the present case, the formation of the transport barrier is dominated by the reduction of diffusivity.

6. Summary and Discussion

We have been constructing a transport model including the effect of the 2-D structure to reveal the self-consistent mechanism of the density pedestal formation in an L/H transition. The electric field structure has steep gradients both in the radial and poloidal directions, which was obtained by solving the model equation including the poloidal structural formation with that giving the time evolution of the radial electric field. The analyses were carried out on L/H transitions induced either spontaneously or by externally forced biasing. The calculation confirms the existence of the 2-D steep structure in the H-mode transport barrier. The 2-D structure affects the density profile by inducing ion and electron fluxes in the radial direction. The ion flux is associated with the radial current to modify the radial electric field, especially in the spontaneous H mode. The electron $E \times B$ flow is cancelled by the diamagnetic flow with Boltzmann electrons, but if there is a phase delay between the potential and density, it can contribute to the formation of the density profile.

In this study, we found that the effect of the 2-D electric field structure does not change the quantitative understanding of the H-mode transition, which has been established by focusing on the 1-D steep gradient of the radial electric field. The quantitative difference

appears in the width of the barrier. The 2-D effect makes the layer of the steep electric field narrower, enhancing the stabilization of micro-turbulence. Next, for the steep density pedestal formation in H-mode transport barriers, two components must be highlighted. One is the reduction of turbulent diffusivity by the steep gradient of the radial electric field, and the other is the increase of the convective fluxes by the formation of the 2-D electric field. The former mechanism has been mainly studied to clarify radial structures in H modes, but this reduced diffusion gives a transition taking much longer time to reach a steady state than observed on the onset of the L/H transition. The generation of a particle pinch associated with the poloidal shock structure can give a rapid density increase if the phase difference δ is substantial. The time constant of the M_p evolution is less than 1 [ms], as shown in Fig. 7, which is characterized by the poloidal transit time t_p . The time constant of the density evolution is ~ 10 ms, which is characterized by the diffusion term in Eq. (9), but the convection, which evolves with the time scale of the electric field, is large enough to affect particle transport in the ramping up phase $t = 0 - 0.2$ [ms] with δ in the range of 0.5. Figure 10 shows the time evolution of the amount of the density increase $\Delta n_0(t) = n_0(t) - n_0(0)$ normalized by that in the final state Δn_H , where n_0 is the density at $r - a = 5$ [cm] (the inner boundary position). The difference in the time evolution of M_p is small, but ramping up speed of $\Delta n_0(t) / \Delta n_H$ is 1.1 times larger in the case with $\delta = 0.5$ than that with $\delta = 0$. Existence of the 2-D structure can accelerate the density evolution. Thus, this convective particle flux is a new candidate for the cause of the rapid establishment of the density pedestal after the onset of the L/H transition.

Acknowledgements

Authors acknowledge discussions with Prof. S.-I. Itoh, Prof. M. Yagi, Prof. A. Fukuyama, Prof. Y. Takase, Prof. Y. Miura, Prof. G. R. Tynan, and Prof. P. Helander. This work is partly supported by the Grant-in-Aid for Specially-Promoted Research of MEXT (16002005), by the Grant-in-Aid for Scientific Research of MEXT (15360495), by Research Fellowships of the Japan Society for the Promotion of Science for Young Scientists, and by the collaboration programs of NIFS and of RIAM of Kyushu University.

-
- [1] WAGNER, F., et al., Phys. Rev. Lett. **49** (1982) 1408.
 - [2] ITOH, K., ITOH, S.-I., FUKUYAMA, A., *Transport and Structural Formation in Plasmas* (IOP, Bristol, 1999).
 - [3] WAGNER, F., et al., in *Proc. of the 13th International Conference on Plasma Physics and Controlled Nuclear Fusion Research, Washington, 1990* (IAEA, Vienna, 1991) Vol. 1, p. 277.
 - [4] TANIUTI, T., MORIGUCHI, H., ISHII, Y., WATANABE, K., WAKATANI, M., J. Phys. Soc. Jpn. **61** (1992) 568.
 - [5] SHAING, K. C., HAZELTINE, R. D., SANUKI, H., Phys. Fluids B **4** (1992) 404.
 - [6] KASUYA, N., ITOH, K., J. Plasma Fusion Res. **81** (2005) 553.
 - [7] SHAING, K. C., CRUME, E. C., HOULBERG, W. A., Phys. Fluids B **2** (1990) 1492.
 - [8] KASUYA, N., ITOH, K., TAKASE, Y., Nucl. Fusion **43** (2003) 244.
 - [9] KASUYA, N., ITOH, K., Phys. Plasmas **12** (2005) 090905.
 - [10] TAYLOR, R. J., et al., Phys. Rev. Lett. **63** (1989) 2365.
 - [11] WEYNANTS, R. R., et al., Nucl. Fusion **32** (1992) 837.
 - [12] ITOH, K., ITOH, S.-I., YAGI, M., FUKUYAMA, A., Phys. Plasmas **5** (1998) 4121.
 - [13] ITOH, S.-I. and ITOH, K., Phys. Rev. Lett. **60** (1988) 2276.
 - [14] SHAING, K. C., CRUME, E. C., Phys. Rev. Lett. **63** (1989) 2369.